Kinetics of Iodine-123-BMIPP in Patients with Prior Myocardial Infarction: Assessment with Dynamic Rest and Stress Images Compared with Stress Thallium-201 SPECT

Ichiro Matsunari, Takashi Saga, Junichi Taki, Yorihiro Akashi, Jun-ichi Hirai, Takanobu Wakasugi, Takahiko Aoyama, Munetaka Matoba, Kenji Ichiyanagi and Kinichi Hisada

Departments of Radiology and Internal Medicine, Fukui Prefectural Hospital, Fukui; Department of Nuclear Medicine, Kanazawa University School of Medicine, Kanazawa, Japan

Myocardial kinetics of ^{123}I-labeled 15-(p-iodophenyl)3R, S-methylpentadecanoic acid (BMIPP) were evaluated with dynamic SPECT, and stress and rest BMIPP images were directly compared in conjunction with stress ^{201}Tl. **Methods:** We studied 26 patients with prior myocardial infarction. Two minutes after injection of BMIPP, dynamic data acquisition with a three-headed SPECT was started and continued for 12 min. Conventional SPECT images were obtained at 20 min and 3 hr after injection. On a separate day, exercise, stress ^{201}Tl SPECT was performed at 10 min and 3 hr after injection. Exercise stress-BMIPP imaging was performed in 15 of the patients, and static SPECT images were obtained. **Results:** With dynamic SPECT, early clearance of BMIPP from the myocardium was observed in the segments with reversible ^{201}Tl defects, suggesting enhanced contribution of backdiffusion from BMIPP. In myocardial segments with reversible ^{201}Tl defects, 20-min BMIPP images showed a higher frequency of reduced uptake when compared to 3-hr ^{201}Tl (90/163) imaging. **Conclusion:** With BMIPP dynamic SPECT, an enhanced contribution of backdiffusion in the early phase from ischemic myocardium was suggested. When exercise stress BMIPP images were obtained, a more severe defect was observed than on rest BMIPP and stress ^{201}Tl imaging, possibly due to decreased coronary blood flow and impaired fatty acid uptake induced by ischemia during exercise.

Key Words: iodine-123-BMIPP; dynamic SPECT; myocardial infarction; exercise thallium-201 imaging

J Nucl Med 1994; 35:1279–1285

Fatty acids are known to play a major role as cardiac energy sources under normal aerobic conditions (*1,2*). The development of fatty acid analogs labeled with radionuclides such as ^{11}C (*3–6*) and ^{123}I (*7–10*) has been encouraged for noninvasive evaluation of myocardial fatty acid metabolism. Structurally modified fatty acids that exhibit normal cardiac extraction, but are not catabolized through the oxidative chain, have been designed for SPECT imaging since their prolonged myocardial retention is appropriate for the longer data acquisition periods required for tomographic imaging. Iodine-123 15-(p-iodophenyl)3R, S-methylpentadecanoic acid (BMIPP) has been proposed as a fatty acid probe for myocardial fatty acid utilization (*11–13*). Several investigators have used modified fatty acids, including BMIPP, in animal models and patients with hypertensive heart disease (*14,15*), cardiomyopathy (*16–19*) and ischemic heart disease (*20–23*). However, the kinetics of injected BMIPP in normal, ischemic or fibrotic myocardium have not yet been elucidated.

Recently, Chouraqui et al. (*24*) compared a labeled modified fatty acid and ^{201}Tl planar imaging in patients with stress-induced ischemia. However, direct comparison of stress and rest modified fatty acid imaging in relation to ^{201}Tl has not been reported.

The objectives of this study were to evaluate the kinetics of BMIPP in normal, ischemic and fibrotic myocardium determined by exercise-redistribution ^{201}Tl imaging with dynamic SPECT imaging in addition to conventional static-SPECT and to compare stress and rest BMIPP imaging in conjunction with stress ^{201}Tl in patients with previous myocardial infarction.

MATERIALS AND METHODS

Patients

Twenty-six patients with previous myocardial infarction (23 men and 3 women), ranging in age from 35 to 83 yr (mean 62.7 yr) were studied (Table 1). The diagnosis was made based on a history of acute myocardial infarction by elevation of cardiac enzymes, typical precordial symptoms and Q-waves on the ECG. The interval from the most recent onset of infarction to the present study ranged from 30 days to 10 yr (mean 18.6 mo). Patients within 4 wk from the onset of infarction were excluded because the metabolic conditions of these patients may be different from those with old myocardial infarction (*23*). Two of the

Received Sept. 29, 1993; revision accepted Mar. 9, 1994.
For correspondence and reprints contact: Ichiro Matsunari, MD, Department of Radiology, Fukui Prefectural Hospital, 2-8-1, Yotsui, Fukui-city, 910, Japan.

TABLE 1
Patient Characteristics

Patient no.	Age	Sex	Infarcted area	Interval* (days)	Preceding intervention
1	70	M	Inferolateral	39	
2	64	M	Inferolateral	485	
3	46	M	Anteroseptal	55	
4	43	M	Anterior	2250	
5	72	M	Inferior	80	PTCA
6	69	M	Anterior	2668	
7	75	M	Inferior	1896	
8	61	F	Inferior	33	
9	40	M	Anteroseptal	154	
10	65	M	Anterior-septal	33	
11	60	M	Anterior-septal	428	PTCA
12	60	M	Inferior, anterior	2127	CABG
13	56	M	Anterior	32	
14	83	M	Inferior	38	
15	70	M	Anterior	62	
16†	58	M	Anteroseptal	34	
17†	62	M	Anteroseptal	34	
18†	70	M	Anteroseptal	40	
19†	52	M	Lateral	45	
20†	78	M	Inferoposterior	32	
21†	73	M	Anterior	56	
22†	35	M	Anteroseptal	36	
23†	67	M	Anterior	30	
24†	63	F	Anteroseptal	3583	
25†	66	F	Inferior	36	
26†	71	M	Inferior	33	

*Interval from the most recent onset of infarction to time of study.
†Stress BMIPP imaging was not performed.
PTCA = percutaneous transluminal angioplasty and CABG = coronary arterial bypass grafting.

patients underwent percutaneous transluminal coronary angioplasty, and one had coronary artery bypass grafting prior to the study. Fifteen patients had stress/rest BMIPP and stress ^{201}Tl studies; the remaining 11 had only rest BMIPP and stress ^{201}Tl studies. All patients gave informed consent in accordance with the hospital's Human Clinical Study Committee guidelines prior to participation in the study.

Radiopharmaceuticals

BMIPP, a beta-methyl-branched fatty acid analog, was prepared and supplied by Nihon Medi-Physics Company. Thallium-201 was obtained from a commercial laboratory.

Instrumentation

A three-headed SPECT system (GCA9300A/HG, Toshiba, Tokyo, Japan) was used for dynamic and static SPECT data acquisition. Data were recorded with low-energy, high-resolution, parallel-hole collimators. The detector system was interfaced to a dedicated nuclear medicine computer.

Imaging Protocol and Data Acquisition

On the day of each radionuclide study patients were instructed to refrain from eating until completion of the study. Each of the resting BMIPP images, including dynamic SPECT, stress BMIPP and stress ^{201}Tl studies, was performed on a separate day. Simultaneous administration and dual-energy acquisition were avoided because of the complexity of crosstalk fraction between ^{123}I and ^{201}Tl (*25*). The study period averaged 11.4 days and ranged from 4 to 21 days. No cardiac events or changes in hemodynamic status occurred during the study period.

Rest BMIPP. Each patient was injected with 111–148 MBq of BMIPP during resting conditions followed by a 20-ml saline flush via an intravenous cannula inserted before the start of the study. From 2 min after injection, dynamic data acquisition was performed with continuous rotation (*26,27*); images were recorded at 4° intervals in 64 × 64 matrices. The camera rotation of 120° around the chest in 120 sec covered the projections over 360°. A total of six series of projection data (2-min data) acquired during a 12-min period were stored on magnetic disks. The energy discrimination was centered on 159 keV with a 20% window.

After dynamic data acquisition, conventional SPECT acquisition was started 20 min after injection (resting 20-min BMIPP). A total of 60 projection images were obtained over 360° in 6° increments with 30 sec per view. The data were recorded in 128 × 128 matrices on the magnetic disk. Conventional SPECT acquisition was also performed 3 hr after injection (resting 3-hr BMIPP) using the same imaging protocol for 20-min BMIPP SPECT.

To reconstruct transaxial tomographic images from each of the dynamic, 20-min and 3-hr BMIPP acquisition data, Butterworth and ramp filters were employed. The parameter of the Butterworth filter was order 8 for each dataset, and the cutoff frequency was 0.19 cycle/pixel for dynamic acquisition data and 0.15 cycle/pixel for conventional SPECT acquisition data. Short-axis slices, 6.4 mm thick for the dynamic and 3.2 mm thick for the conventional SPECT acquisition data, were also generated. Two serial slices of conventional SPECT data were added to equalize the slice thickness of the dynamic SPECT data.

Stress BMIPP. In 15 patients, exercise stress BMIPP imaging was performed using a supine bicycle ergometer. Exercise was started with a workload of 25 W and increased by 25 W intervals for every 2 min of stress. Exercise was terminated when either severe chest pain, serious arrhythmia, ST depression of more than 0.2 mV and/or fatigue occurred. One minute before cessation of exercise, 111–148 MBq of BMIPP were injected and 20-min and 3-hr SPECT images were obtained using the same protocol for resting BMIPP.

Stress ^{201}Tl SPECT. Exercise stress ^{201}Tl SPECT imaging was also performed using a supine bicycle ergometer. At the same workload level used in the stress BMIPP study, approximately 111 MBq of ^{201}Tl were injected intravenously, and the patient continued to exercise for an additional minute. At 10 min and 3 hr after injection, exercise and 3-hr SPECT images were obtained under the same acquisition conditions and reconstruction method used for BMIPP SPECT, except the energy discriminator was centered on 70 keV with a 20% window.

Data Analysis

SPECT data analysis was based on three reconstructed short-axis slices. In each patient, corresponding short-axial tomograms from the sets of dynamic SPECT with BMIPP, 20-min and 3-hr BMIPP SPECT and exercise and 3-hr ^{201}Tl SPECT were aligned, and three slices from the basal, middle and apical ventricular levels were chosen for direct comparison. Basal and middle ventricular slices were divided into eight segments, and the apical ventricular slice was divided into four segments (Fig. 1). A square region of interest (ROI) of 3 × 3 pixels for dynamic SPECT or 6 × 6 pixels for conventional SPECT was placed over the center of each of the total 20 segments. Thus, a total of 520 myocardial segments from 26 patients were evaluated.

The washout rate from 2–4 to 12–14 min images was calculated in each myocardial segment. Physical decay correction was not made for dynamic SPECT data, since it was considered negligible during the short acquisition time.

In each SPECT datum, the maximum value (average counts per pixel) of all 20 myocardial segments was taken as 100%; the other values were calculated as a percentage of this maximum (relative regional uptake, RRU). For quantitative analysis of the SPECT data, a five-point scoring system based on RRU was used in each myocardial segment: 4 (RRU, 80%–100%), 3 (60%–79%), 2 (40%–59%), 1 (20%–39%) and 0 (0%–19%).

On the basis of the five-point scoring system for ^{201}Tl studies, the myocardial segments were classified into three patterns as follows:

Normal: a segment showing a score of 4 on both exercise and 3-hr ^{201}Tl images.

Reversible defect: a segment showing a lower score on exercise ^{201}Tl images than on 3-hr ^{201}Tl images.

Nonreversible defect: a segment showing a score of less than 4 on 3-hr ^{201}Tl images and an equal or larger score on exercise ^{201}Tl images.

In addition, the washout rates (%) in ^{201}Tl and BMIPP studies were calculated in each segment (physical decay-corrected).

Statistical Analysis

Values are expressed as mean ± s.e.m.. A paired t-test was used only to compare the washout rates of corresponding myocardial segments between stress and rest BMIPP study. For other comparisons of mean values, the F-test was applied. Linear regression analysis was performed to determine the correlation between washout rates calculated from 2–4 to 12–14 min and from 20 min to 3 hr BMIPP SPECT. Chi-square analysis was used to determine differences in proportions of resting 20-min-BMIPP/3-hr ^{201}Tl discrepancy. McNemar's symmetry chi-square was used to compare the conventional SPECT images. Statistical significance was defined as $p < 0.05$.

RESULTS

Classification of Myocardial Segments by Exercise Redistribution ^{201}Tl SPECT

Of a total 520 myocardial segments, 170 were classified as normal, 163 as reversible defects and 187 as nonreversible defects by quantitative analysis. All patients had positive scintigraphic findings on both exercise and 3-hr ^{201}Tl imaging.

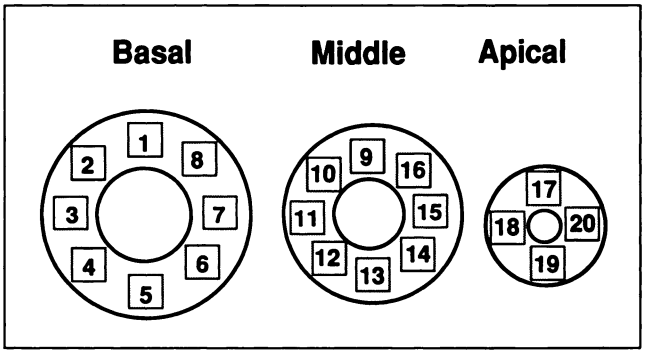

FIGURE 1. Three reconstructed short-axis slices in the basal, middle and apical ventricle. Eight square ROIs of 3 × 3 pixels for dynamic SPECT or 6 × 6 pixels for static SPECT were placed on the basal and middle slices, and four square ROIs were placed on the apical slice.

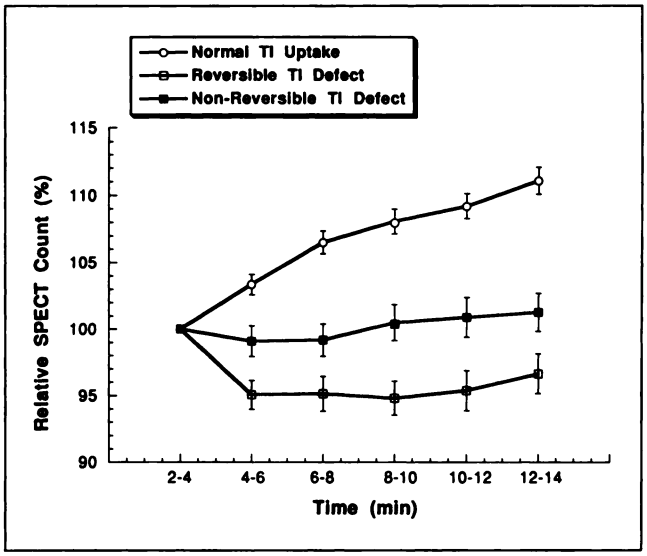

FIGURE 2. Time-activity curves of BMIPP from 2–4 to 12–14 min in myocardial segments with normal ^{201}Tl uptake, reversible ^{201}Tl defects and nonreversible ^{201}Tl defects. The first datapoints are standardized to 100%. Mean and s.e.m. are shown.

Early Kinetics of Rest Injected BMIPP in Dynamic SPECT

For the dynamic SPECT study, BMIPP washout rates (from 2–4 to 12–14 min) of myocardium with reversible ^{201}Tl defects (3.6 ± 1.5%) was higher than those with normal ^{201}Tl uptake and nonreversible ^{201}Tl defects (−11.1 ± 1.0%, $p < 0.001$, and −1.2 ± 1.4%, $p < 0.05$, respectively). The dynamic, early time-activity curves from 2–4 to 12–14 min showed a subsequent decrease of BMIPP activity in the reversible ^{201}Tl defect area, while a subsequent increase of BMIPP activity in normal ^{201}Tl uptake and no significant change in BMIPP activity in nonreversible ^{201}Tl defect areas were noted (Fig. 2).

Figure 3 shows a representative case comparing exercise-redistribution ^{201}Tl SPECT, resting 20-min BMIPP SPECT and BMIPP dynamic SPECT. Exercise, redistribution ^{201}Tl SPECT shows a reversible defect pattern in the septal wall and resting 20-min BMIPP shows decreased uptake compared with 3-hr ^{201}Tl. In BMIPP dynamic SPECT, clearance in the septal region is noted.

Of note, the washout rate calculated from dynamic SPECT was not positively correlated with 20-min to 3 hr BMIPP SPECT results, showing only a weak negative correlation ($r = -0.249$, $p < 0.001$) (Fig. 4).

Comparison Between Rest BMIPP and Stress ^{201}Tl Imaging

As shown in Figure 5, 20-min BMIPP imaging showed reduced activity compared to 3-hr ^{201}Tl ($p < 0.001$). On the other hand, exercise ^{201}Tl showed reduced activity compared with 20-min BMIPP ($p < 0.005$). In myocardial seg-

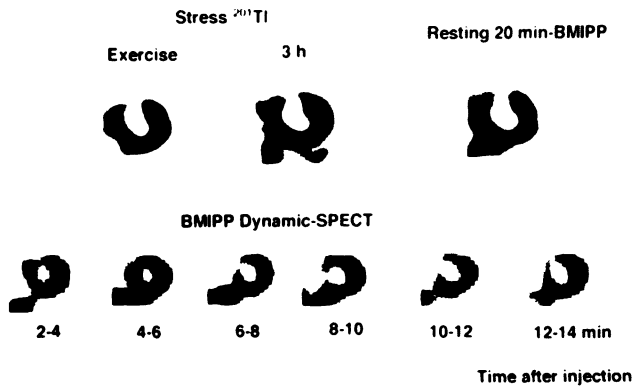

FIGURE 3. (Upper) Short-axis tomograms of exercise-redistribution ^{201}Tl SPECT and resting 20-min BMIPP SPECT of Patient 11 with anterior and septal wall infarction. The exercise-redistribution ^{201}Tl images show a reversible defect in the septal wall. On resting 20-min BMIPP SPECT, decreased BMIPP uptake compared with 3-hr ^{201}Tl in the septal wall is observed. (Lower) serial changes in the accumulation pattern in BMIPP dynamic SPECT of the same patient as shown above are observed. A significant clearance of BMIPP from the septal wall is noted.

ments with reversible ^{201}Tl defects, 20-min BMIPP showed a high frequency of reduced uptake compared to 3-hr ^{201}Tl (90 of 163 myocardial segments), whereas segments with normal ^{201}Tl uptake and nonreversible ^{201}Tl defects showed a relatively low frequency of lower BMIPP uptake than ^{201}Tl (16 of 170 and 29 of 187 segments) (Table 2).

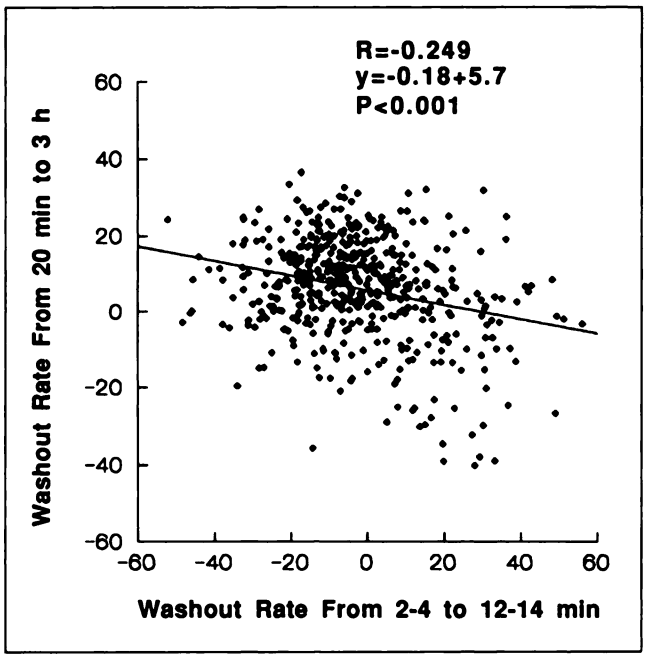

FIGURE 4. Correlation of washout rate between BMIPP dynamic SPECT (from 2–4 to 12–14 min) and resting BMIPP SPECT (from 20 min to 3 hr). A very weak negative correlation was observed.

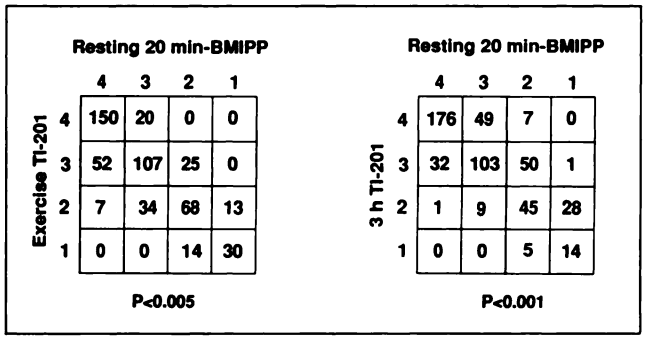

FIGURE 5. Comparison of uptake scores between resting 20-min BMIPP and exercise ^{201}Tl imaging (left) and between resting 20-min BMIPP and 3-hr ^{201}Tl imaging (right).

Comparison of Stress BMIPP and Rest BMIPP in Relation to Stress ^{201}Tl

Comparisons of segmental uptake scores between stress 20-min BMIPP and resting 20-min BMIPP SPECT and between stress 20-min BMIPP and exercise ^{201}Tl SPECT are shown in Figure 6. There were no segments with a score of 0 (<20%, RRU), both in BMIPP and ^{201}Tl. The stress 20-min BMIPP exhibited more severe defects when compared with resting 20-min BMIPP ($p < 0.001$). Furthermore, defects on stress 20-min-BMIPP were more severe compared to exercise ^{201}Tl ($p < 0.05$).

The stress, 3-hr BMIPP showed a high frequency of redistribution ($p < 0.001$), whereas resting 3-hr BMIPP did not (Fig. 7). The washout rate calculated from stress BMIPP, rest BMIPP and stress ^{201}Tl in segments with normal ^{201}Tl uptake and reversible and nonreversible ^{201}Tl defects are summarized in Table 3. In normal ^{201}Tl uptake segments, the washout rates of BMIPP (both stress and rest study) were higher segments with reversible and nonreversible ^{201}Tl defects. In addition, the washout rate of stress BMIPP in the segments with normal ^{201}Tl uptake was higher than rest BMIPP ($p < 0.05$).

Figure 8 shows short-axis images of stress ^{201}Tl, rest BMIPP and stress BMIPP of a representative case of inferolateral wall myocardial infarction. The most severe de-

TABLE 2
Resting Twenty Minute BMIPP/Three Hour ^{201}Tl Discrepancies in Relation to Exercise-Redistribution ^{201}Tl Patterns (Number of Segments)

	Normal	Reversible defect	Nonreversible defect	Total
BMIPP < Tl*	16	90	29	135
BMIPP = Tl†	154	67	117	338
BMIPP > Tl‡	0	6	41	47
Total	170	163	187	520

*Segments with lower BMIPP uptake than ^{201}Tl.
†Segments with equal uptake of BMIPP and ^{201}Tl.
‡Segments with lower ^{201}Tl uptake than BMIPP.
$p < 0.001$.

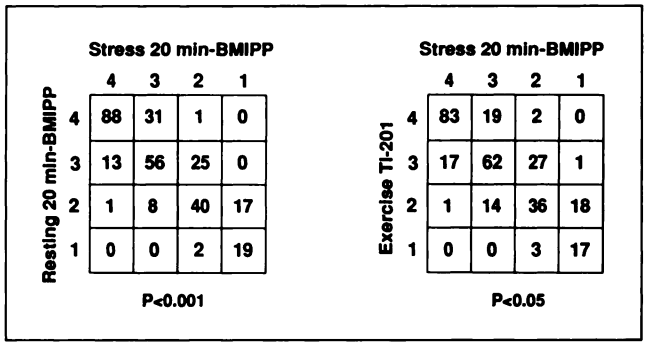

FIGURE 6. Comparison of segmental uptake scores between stress 20-min BMIPP and resting 20-min BMIPP imaging (left) and between stress 20-min BMIPP and exercise ^{201}Tl imaging (right).

fect was seen on the stress 20-min BMIPP image; the 3-hr image showed a less severe defect in this region.

DISCUSSION

We noted the following observations during this study:

1. For dynamic SPECT, relatively increased clearance of BMIPP from the myocardium was observed in segments with reversible ^{201}Tl defects.
2. Abnormal resting BMIPP uptake was more frequently observed than in 3-hr ^{201}Tl imaging.
3. In segments with nonreversible ^{201}Tl defects, a majority of segments showed equally decreased resting 20-min BMIPP and 3-hr ^{201}Tl uptake, whereas in segments with reversible ^{201}Tl defects, the resting 20-min BMIPP defects were frequently more severe than those on 3-hr ^{201}Tl images.
4. BMIPP defects were more prominent on the stress studies than resting studies, and stress 20-min BMIPP showed more severe defects than exercise ^{201}Tl.

Early Kinetics of BMIPP

We demonstrated early clearance of BMIPP from the myocardium with reversible ^{201}Tl defects in the dynamic study. Since methyl-branched fatty acid analogues, including BMIPP, are thought not to enter the beta-oxidation

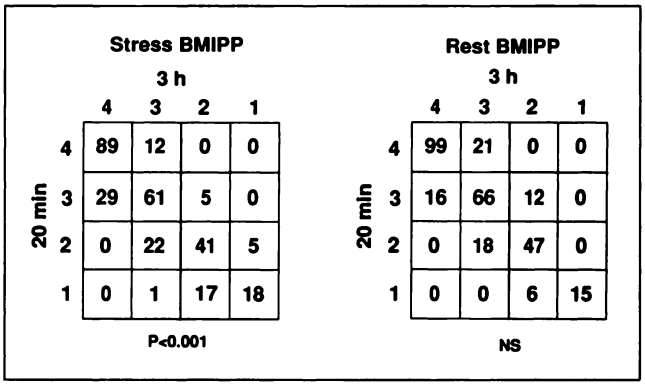

FIGURE 7. Comparison of segmental uptake scores between 20-min and 3-hr imaging on stress (left) and rest (right) BMIPP study.

TABLE 3
Washout Rates for Stress, Rest BMIPP and Stress ^{201}Tl in Segments with Normal, Reversible and Nonreversible Defects in Stress ^{201}Tl Studies

Stress finding ^{201}Tl study	Stress BMIPP	Rest BMIPP	Stress ^{201}Tl
Normal (n = 104)*	15.8 ± 0.8†	13.0 ± 1.0	39.6 ± 0.7
Reversible defect (n = 77)*	4.0 ± 1.4‡§	5.6 ± 1.4§	27.1 ± 1.4¶
Nonreversible defect (n = 119)*	7.8 ± 1.2§	6.4 ± 1.4§	38.8 ± 0.8

Results (mean ± s.e.m.) are percent washout from 20 min to 3 hr for rest and stress BMIPP; percent washout from 10 min to 3 hr for stress ^{201}Tl.
*Classification was determined by stress ^{201}Tl.
†$p < 0.05$ vs. rest BMIPP.
‡$p < 0.05$ vs. nonreversible defect.
§$p < 0.001$ vs. normal.
¶$p < 0.001$ vs. normal and nonreversible defect.

catabolic pathway, it is improbable that BMIPP trapped by the myocardium could be rapidly metabolized. Therefore, accelerated clearance of BMIPP in the early dynamic phase just after the injection of BMIPP (2–14 min) in myocardial segments with reversible ^{201}Tl defects indicating ischemic myocardium might be explained by backdiffusion. Fox et al. measured the efflux of metabolized and nonmetabolized fatty acid from canine myocardium using ^{11}C-palmitate and showed a significant increase of backdiffusion with either ischemia or hypoxia during the interval from 1 to 10 min after tracer injection (*28*). Lerch also observed enhanced backdiffusion of injected ^{123}I-heptadecanoic acid (HDA) from isolated rabbit hearts during hypoxia (*29*). The mechanism of BMIPP backdiffusion might be explained as follows. In the metabolically impaired myocardium conversion of BMIPP to BMIPP-CoA might be suppressed, and so free BMIPP, which is distributed by

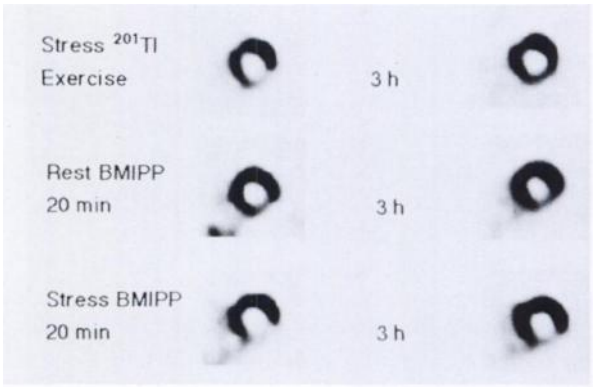

FIGURE 8. Short-axis tomograms of Patient 1 with inferolateral infarction. A defect in the inferolateral wall was observed on exercise ^{201}Tl, which was accompanied by incomplete redistribution on 3-hr ^{201}Tl images (upper row). The defect on resting 20-min BMIPP imaging was more severe than on 3-hr ^{201}Tl (middle row). The most severe defect was seen on stress 20-min BMIPP, which was accompanied by redistribution on the 3-hr BMIPP image (lower row).

regional perfusion, cannot be retained in the myocardial cell in a similar mechanism shown in the studies using ^{11}C-palmitate and ^{123}I-HDA. On the other hand, myocardial segments exhibiting either a normal or nonreversible defect showed a subsequent increase in BMIPP uptake during dynamic SPECT imaging. Dudczak et al. reported that the activity peak time of injected BMIPP in the human heart averaged 14.9 min (*13*), which is consistent with our findings. In these myocardial regions, the contribution of backdiffusion is considered to be low, and the trapped BMIPP is incorporated into the endogenous lipid pool.

Notably, the washout rate from 2–4 to 12–14 min and from 20 min to 3 hr did not show any positive correlation, indicating that the backdiffusion observed here is independent of BMIPP washout from 20 min to 3 hr images. Mechanisms other than backdiffusion, such as alpha-oxidation, may contribute to washout from myocardium from 20 min to 3 hr. Judging from the time-activity curves obtained by dynamic SPECT, a considerable part of backdiffusion may be completed within 6 min, an interpretation in agreement with findings by Fox et al. (*28*).

It was difficult to clarify the contribution of backdiffusion of fatty acids or their analog such as ^{11}C-palmitate or 15-(para-^{123}I-phenyl) pentadecanoic acid with external imaging modalities because of the coexistence of beta-oxidation and backdiffusion (*30*). Because of their resistance to metabolism by beta-oxidation, methyl-branched fatty acids such as BMIPP permit estimation of backdiffusion when dynamic SPECT is used.

Comparison Between Resting 20-min BMIPP and Exercise-Redistribution ^{201}Tl SPECT

Resting 20-min BMIPP showed reduced activity in comparison to 3-hr ^{201}Tl, especially in the region of reversible defects on exercise-redistribution ^{201}Tl imaging (90/163 Segments, 55%). This indicates that impaired fatty acid utilization already exists during resting conditions in stress-induced ischemic myocardium. Thus, resting BMIPP imaging, in combination with exercise-redistribution ^{201}Tl imaging, is useful in obtaining precise information on myocardial injury.

Comparison of Stress and Rest BMIPP SPECT in Conjunction with Stress ^{201}Tl

We demonstrated that exercise stress BMIPP imaging exhibits a more serious defect than rest BMIPP and stress ^{201}Tl in patients with prior myocardial infarction. Kaiser et al. compared stress- and rest-SPECT imaging with 15-(ortho-^{123}I-phenyl)-pentadecanoic acid and a subtraction method and observed fill-in in myocardium showing diminished tracer uptake after exercise (*33*). Their results are consistent with ours. On the other hand, Chouraqui et al. compared a fatty acid analogue and ^{201}Tl imaging in patients with stress-induced ischemia, resulting in good agreement with both tracers (*24*). The mechanism of the most severe defects seen on stress BMIPP SPECT in the stress and rest BMIPP studies and the ^{201}Tl studies may be due to decreased BMIPP delivery by reduced coronary blood flow and impaired fatty acid uptake by exercise-induced ischemia.

Primarily, BMIPP is designed to inhibit beta-oxidation. However, considerable myocardial clearance still exists, possibly due to catabolism by alpha- or omega-hydroxylation with subsequent oxidation (*34,35*). Moreover, the frequency of redistribution on 3-hr imaging was significantly high in the stress BMIPP SPECT study, which is consistent with previous work (*24*). The frequent redistribution observed on stress 3-hr-BMIPP SPECT could be explained by increased washout from normal myocardium, whereas defects are accompanied by persistently reduced washout. The increased clearance of BMIPP by exercise stress may not be explained by increased coronary arterial blood flow, since it seems to return to baseline levels at 15 min after the end of exercise (*36*). Some metabolic change after exercise might influence the washout rate from 20-min to 3-hr images.

Methodological Limitations

In the present study, we employed ^{201}Tl redistribution images after exercise stress under resting conditions. However, recent studies have shown that reinjection of thallium after redistribution imaging may result in enhanced thallium uptake within apparently irreversible thallium defects (*31,32*). Thus, 3-hr ^{201}Tl imaging may underestimate viable myocardium. Therefore, the possibility exists that myocardial segments showing nonreversible defects may actually contain viable myocardium and cannot be excluded in this study.

CONCLUSIONS

We used dynamic SPECT to demonstrate significant clearance of BMIPP from myocardium with reversible ^{201}Tl defects in the early phase, suggesting enhanced contribution of backdiffusion in ischemic myocardium. Resting 20-min BMIPP imaging frequently demonstrated more decreased tracer uptake than 3-hr ^{201}Tl imaging in ischemic myocardium, implicating impaired fatty acid metabolism during resting conditions. When exercise-stress BMIPP images were obtained, more severe defects were observed than on rest BMIPP and stress ^{201}Tl images, possibly due to decreased coronary blood flow and impaired fatty acid uptake induced by ischemia during exercise.

ACKNOWLEDGMENTS

The authors thank Mr. Kouichi Ono, Mr. Yoshinobu Tanishima and Ms. Hiroko Nishide of the Radioisotope Division for their assistance. BMIPP was kindly supplied by Nihon Medi-Physics Co., Ltd., Nishinomiya, Japan.

REFERENCES

1. Opie LH. Metabolism of the heart in health and disease. *Am Heart J* 1968;76:685.
2. Neely JR, Rovetto MJ, Oram JF. Myocardial utilization of carbohydrate and lipids. *Prog Cardiovasc Dis* 1972;15:685–698.
3. Sobel BE, Weiss ES, Welch MJ, Siegel BA, Ter-Pogossian MM. Detection of remote myocardial infarction in patients with positron emission transaxial tomography. *Circulation* 1977;55:853–857.

4. Lerch RA, Bergmann SR, Ambos HD, Welch MJ, Ter-Pogossian MM, Sobel BE. Effect of flow-independent reduction of metabolism on regional myocardial clearance of ^{11}C-palmitate. *Circulation* 1982;65:731–738.
5. Schon HR, Schelbert HR, Robinson G, et al. Carbon-11-labeled palmitic acid for the noninvasive evaluation of regional myocardial fatty acid metabolism with positron-computed tomography. I. Kinetics of C-11 palmitic acid in normal myocardium. *Am Heart J* 1982;103:532–547.
6. Schon HR, Schelbert HR, Najafi A, et al. Carbon-11-labeled palmitic acid for the noninvasive evaluation of regional myocardial fatty acid metabolism with positron-computed tomography. II. Kinetics of C-11 palmitic acid in acutely ischemic myocardium. *Am Heart J* 1982;103:548–561.
7. van der Wall EE, Heidendal GAK, den Hollander W, Westera G, Roos JP. I-123-labeled hexadecanoic acid in comparison with thallium-201 for myocardial imaging in coronary artery disease. *Eur J Nucl Med* 1983;6:391–396.
8. Shon HR, Senekowitsch R, Berg D, et al. Measurement of myocardial fatty acid metabolism: kinetics of iodine-123-heptadecanoic acid in normal dog hearts. *J Nucl Med* 1986;27:1449–1455.
9. Machulla HJ, Marsmann M, Dutschka K. Biochemical concepts and synthesis of radioiodinated phenyl fatty acid for in vivo metabolic studies of the myocardium. *Eur J Nucl Med* 1980;5:171–173.
10. Rellas JS, Corbett JR, Kulkarni P, et al. Iodine-123 phenylpentadecanoic acid: detection of acute myocardial infarction and injury in dogs using an iodinated fatty acid and single-photon emission tomography. *Am J Cardiol* 1983;52:1326–1332.
11. Goodman MM, Kirsch G, Knapp FF Jr. Synthesis and evaluation of radioiodinated terminal p-iodo-phenyl-substituted alpha- and beta-methyl-branched fatty acids. *J Med Chem* 1984;27:390–397.
12. Knapp FF Jr, Ambrose KR, Goodman MM. New radioiodinated methyl-branched fatty acids for cardiac studies. *Eur J Nucl Med* 1986;12:S39–S44.
13. Dudczak R, Schmoliner R, Angelberger P, Knapp FF, Goodman MM. Structurally modified fatty acids: clinical potential as tracers of metabolism. *Eur J Nucl Med* 1986;12:S45–S48.
14. Yonekura Y, Brill AB, Som P, et al. Reginal myocardial substrate uptake in hypertensive rats: a quantitative autoradiographic measurement. *Science* 1985;227:1494–1496.
15. Yamamoto K, Som P, Brill AB, et al. Dual tracer autoradiographic study of beta-methyl-(1-^{14}C) heptadecanoic acid and 15-p-(^{131}I)-iodophenyl-beta-methylpentadecanoic acid in normotensive and hypertensive rats. *J Nucl Med* 1986;27:1178–1183.
16. Kurata C, Kobayashi A, Yamazaki N. Dual tracer autoradiographic study with thallium-201 and radioiodinated fatty acid in cardiomyopathic hamsters. *J Nucl Med* 1989;30:80–87.
17. Kurata C, Tawarahara K, Taguchi T, et al. Myocardial emission computed tomography with iodine-123-labeled beta-methyl-branched fatty acid in patients with hypertrophic cardiomyopathy. *J Nucl Med* 1992;33:6–13.
18. Taki J, Nakajima K, Bunko H, Shimizu M, Taniguchi M, Hisada K. Iodine-123-labeled BMIPP fatty acid myocardial scintigraphy in patients with hypertrophic cardiomyopathy: SPECT comparison with stress ^{201}Tl. *Nucl Med Commun* 1993;14:181–188.
19. Takeishi Y, Chiba J, Abe S, Tonooka I, Komatani A, Tomoike H. Heterogeneous myocardial distribution of iodine-123 15-(p-iodophenyl)-3-R,S-methylpentadecanoic acid (BMIPP) in patients with hypertrophic cardiomyopathy. *Eur J Nucl Med* 1992;19:775–782.
20. Miller DD, Gill JB, Livini E, et al. Fatty acid analogue accumulation: a marker of myocyte viability in ischemic-reperfused myocardium. *Circ Res* 1988;63:681–692.
21. Nishimura T, Sago M, Kihara K, et al. Fatty acid myocardial imaging using ^{123}I-β-methyl-iodophenyl pentadecanoic acid (BMIPP): comparison of myocardial perfusion and fatty acid utilization in canine myocardial infarction (occlusion and reperfusion model). *Eur J Nucl Med* 1989;15:341–345.
22. Saito T, Yasuda T, Gold HD, et al. Differentiation of regional perfusion and fatty acid uptake in zones of myocardial injury. *Nucl Med Commun* 1991; 12:663–675.
23. Tamaki N, Kawamoto M, Yonekura Y, et al. Regional metabolic abnormality in relation to perfusion and wall motion in patients with myocardial infarction: assessment with emission tomography using an iodinated branched fatty acid analog. *J Nucl Med* 1992;33:659–667.
24. Chouraqui P, Maddahi J, Henkin R, Karesh SM, Galie E, Berman DS. Comparison of myocardial imaging with iodine-123-iodophenyl-9-methyl pentadecanoic acid and thallium-201-chloride for assessment of patients with exercise-induced myocardial ischemia. *J Nucl Med* 1991;32:447–452.
25. Nakajima K, Taki J, Bunko H, et al. Errors of uptake in dual energy acquisition with ^{201}Tl and ^{123}I-labeled radiopharmaceuticals. *Eur J Nucl Med* 1990;16:595–599.
26. Nakajima K, Taki J, Bunko H, et al. Dynamic acquisition with a three-headed SPECT system: application to technetium 99m-SQ30217 myocardial imaging. *J Nucl Med* 1991;32:1273–1277.
27. Nakajima K, Shuke N, Taki J, et al. A simulation of dynamic SPECT using radiopharmaceuticals with rapid clearance. *J Nucl Med* 1992;33:1200–1206.
28. Fox KAA, Abendschein DR, Ambos HD, Sobel BE, Bergmann SR. Efflux of metabolized and nonmetabolized fatty acid from canine myocardium: implications for quantifying myocardial metabolism tomographically. *Circ Res* 1985;57:232–243.
29. Lerch R. Effect of impaired fatty acid oxidation on myocardial kinetics of ^{11}C- and ^{123}I-labeled fatty acids. *Eur J Nucl Med* 1986;12:S36–S38.
30. Wieler H, Kaiser KP, Frank J, Kuikka JT, Ladwein K, Winkens A. Standardized non-invasive assessment of myocardial free fatty acid kinetics by means of 15-(para-iodo-phenyl) pentadecanoic acid (^{123}I-pPPA) scintigraphy: I. Method. *Nucl Med Commun* 1990;11:865–878.
31. Dilsizian V, Rocco TP, Freedman NMT, Leon MB, Bonow RO. Enhanced detection of ischemic but viable myocardium by the reinjection of thallium after stress-redistribution imaging. *N Engl J Med* 1990;323:141–146.
32. Rocco TP, Dilsizian V, McKusick KA, Fischman AJ, Boucher CA, Strauss HW. Comparison of thallium redistribution with rest "reinjection" imaging for the detection of viable myocardium. *Am J Cardiol* 1990;66:158–163.
33. Kaiser KP, Vester E, Großmann K, et al. Semiquantitative analysis of SPECT with the iodinated fatty acid 15-(ortho-^{123}I-phenyl)-pentadecanoic acid. *Nucl Med Commun* 1991;12:927–936.
34. Fink GD, Montgomery JA, David F, et al. Metabolism of beta-methyl-heptadecanoic acid in perfused heart and liver. *J Nucl Med* 1990;31:1823–1830.
35. Knapp FF Jr, Goodman MM, Callahan AP, Kirsch G. Radioiodinated 15-(p-iodophenyl)-3,3-dimethylpentadecanoic acid: a useful new agent to evaluate myocardial fatty acid uptake. *J Nucl Med* 1986;27:521–531.
36. Camici P, Araujo LI, Spinks T, et al. Increased uptake of ^{18}F-fluorodeoxyglucose in postischemic myocardium of patients with exercise-induced angina. *Circulation* 1986;74:81–88.